FLEXURAL BEHAVIOR OF FRP REINFORCED CONCRETE PILES

Mousa, S.[1], Mohamed, H. M.[1], and Benmokrane, B.[1]*
[1] Department of civil engineering, University of Sherbrooke, Sherbrooke, Quebec, Canada
* Corresponding author (Brahim.Benmokrane@Usherbrooke.ca)

Keywords*: Flexural, Fiber reinforced polymer, Concrete Piles.*

ABSTRACT

Considerable experimental research work has been conducted to evaluate the flexural strength of rectangular concrete members reinforced with fiber-reinforced polymer (FRP) bars. In contrast, no research seems to have investigated circular concrete members reinforced with FRP bars under flexural loads. This paper reports on a study on the behavior and flexural strength of full-scale circular concrete beams reinforced with longitudinal Glass FRP (GFRP) bars. The beams, which measured 6,000 mm in length by 500 mm in diameter, were tested under four-point bending. Steel and GFRP bars were used in the experimental program. The experimental results were presented in terms of the general behavior of the tested specimens, flexural capacity, crack pattern and mode of failure.

1 INTRODUCTION

Circular reinforced concrete (RC) members are widely used in infrastructure systems, such as bridge piers and piles, contiguous pile walls and fender piling in marine structures. This is due to the simplicity of construction and because their strength characteristics under lateral loads are similar in any direction. These members, in most cases, are exposed to aggressive environments which led to corrosion of reinforcing steel inside the concrete, which causes failure or deterioration of these structures leading to costly repairs and rehabilitation [1], as well a significant reduction in service life of these structures. To avoid such problems, infrastructure owners are looking for new technologies that extend the service live of concrete structures and reduce maintenance costs [2]. The use of fiber reinforced polymers (FRP) has increased during the last two decades. Known to be non-corrosive material, FRP reinforcing bars provides a superior alternative to steel reinforcement. FRP materials have many advantages compared to steel; its density is one-quarter to one-fifth of the steel, neutrality to electrical and magnetic disturbances, and a high tensile strength [3].

In the last two decades, considerable research programs have been carried out to investigate the flexural response of FRP RC members with rectangular sections [4-10]. These studies greatly improving our knowledge of how rectangular concrete members reinforced with FRP bars should be analyzed and designed. Based on that, design equations and limitations were proposed and included in the design guidelines and codes [3, 11-12]. Codes and design guidelines do not usually propose specific formulations or instructions for design and analysis of RC circular members in contrast with its widespread use. In addition, a little attention was given to RC circular members in the literature [13-15]. Moreover, ACI 440.1R-15 [3] highlights that no evidence that the flexural theory, which developed for rectangular sections, does not apply equally well to nonrectangular sections and the behavior of nonrectangular sections has yet to be confirmed by experimental results.

Recently, some studies have investigated the behavior of FRP RC circular members under concentric, eccentric, and shear loading [2, 16-19] as a part of a comprehensive experimental program carried out at the University of

Sherbrooke. In this study, an experimental work on large-scale circular concrete members reinforced with glass FRP (GFRP) bars and spirals tested under four-point bending load was conducted to study its flexural behavior.

2 EXPERIMENTAL PROGRAM

2.1 Materials

The GFRP reinforcements employed in this study were manufactured by pultrusion process. GFRP bars # 6 and GFRP spirals # 4 were used as longitudinal and transverse reinforcement, respectively. The GFRP bars and spirals have a sand-coated surface as shown in Figure 1 to enhance bond and force transfer between bars and concrete. The mechanical properties of the GFRP bars are shown in Table 1 as reported by the manufacturer. Two steel bar diameters were used to reinforce the control specimen. Deformed steel bars No. 20M were used as longitudinal reinforcement and deformed steel bars No. 10M were used as a spiral. Table 1 gives the mechanical proprieties of steel bars used in this study. The two specimens were cast using normal-weight, ready-mixed concrete with a target compressive strength of 40 MPa. The actual compressive strength was 41.43 MPa and determined based on the average test results of 10 concrete cylinders 100 x 200 mm tested on the same day as the start of testing of the specimens.

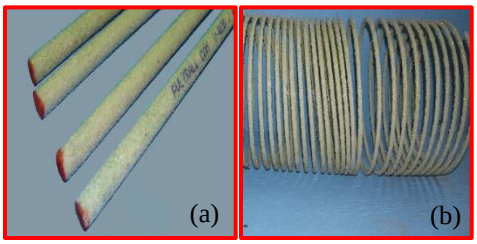

Figure 1: a) GFRP bars and b) GFRP spirals.

Bar Size	Diameter (mm)	Area (mm^2)	Elastic Tensile Modulus (GPa)	Tensile Strength (MPa)	Tensile Strain (%)
GFRP spirals					
# 4	12.7	129	51.4	f_{fu} = 1414	2.75
GFRP bars					
# 6	20	285	63.9	f_{fu} = 1635	2.56
Steel bars					
10M	11.3	100	200	f_y = 460	0.23
20M	20.0	300	200	f_y = 460	0.23

Table 1. Mechanical properties of the GFRP and steel reinforcements

2.2 Test Specimens

A large-scale RC circular specimens, including one reinforced with GFRP bars and spirals and one with steel reinforcement, were prepared and tested. The tested specimens were 500 mm in diameter, and 6000 mm long. The specimens were tested under four-point bending, with 4950 mm clear span and 2100 mm shear span. The distance

between loads was 750 mm. Figure 2 shows the dimensions and reinforcement details of the tested specimens. Table 2 provides the test matrix and reinforcement details of the tested specimens. Each specimen's code was identified with letters and numbers. The first number indicates the number of longitudinal bars. The letters G and S identify specimens as being reinforced totally with GFRP or steel reinforcement, respectively. The second number indicates the nominal diameter of longitudinal bars.

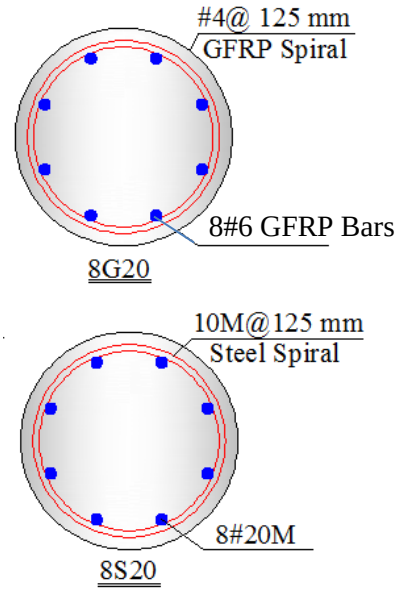

Figure 2: Reinforcement details of the test specimens.

Specimen ID	Reinforcement type	Longitudinal reinforcement		Transversal reinforcement
		ρ_{ft} (%)	Number of bars	
8G20	Glass FRP	1.16	GFRP bars (8 No. 20)	GFRP spiral # 4 @125
8S20	Steel	1.22	Steel bars (8 #20 M)	Steel spiral 10 M @125

Table 2. Test matrix and details of tested specimens

2.3 Test Setup

The test setup was designed and fabricated at the University of Sherbrooke's CFI structural laboratory. Steel saddles were designed to accommodate the circular geometry at loading and support points. The specimens were loaded in four-point bending load, as shown in Figure 3, using a servo-controlled, hydraulic 1000 kN MTS actuator attached to a spreader beam. The load was applied at a displacement-controlled rate of 0.5 mm/min. An automatic data-acquisition system monitored by a computer was used to record the readings.

Figure 3: Test Setup and deflected shape of test specimen

2.4 Test results and discussion

This section summarizes the experimental results, including the general behavior of the tested specimens, flexural capacity, crack pattern and mode of failure.

2.4.1 General Behavior of the Tested Specimens

In this section, the moment-deflection curves at mid-span and quarter-span for the tested specimens are presented in Figure 4. Before cracking, an identical linear moment–deflection behavior was observed for the two tested specimens regardless of their reinforcement type, representing the uncracked condition that governed by the properties of the concrete circular section. After cracking, the response of GFRP specimen was almost linear up to the initiation of concrete crushing at the compression side of the circular cross-section. After that, a sudden load drop occurred, indicating that concrete crushing failure had transpired. Interestingly, the specimens did not lose their load-carrying capacity after concrete crushing. Instead, they continued to sustain additional loads. This behavior can be attributed to the confinement effect provided by the GFRP bars and spirals and the contribution of compression bars that enhanced the specimen ductility and strength. In the case of specimen reinforced with steel bars, the moment-deflection curve shows a typical yielding plateau followed by concrete crushing in the compression zone. Afterward, a sudden load drop evidenced followed by a whole losing of the flexural stiffness of the specimen.

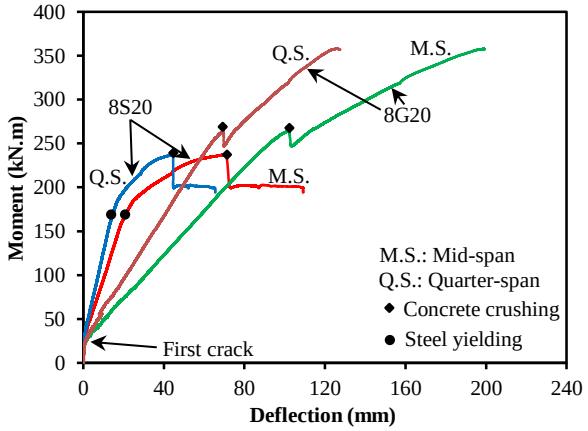

Figure 4. Moment-deflection relationship.

2.4.2 Flexural capacity, crack pattern and mode of failure

Table 3 provides flexural capacity and mode of failure for the tested specimens. The failure of GFRP RC circular specimen occurred by concrete crushing at midspan's compression zone, while the steel RC circular specimen failed due to steel yielding followed by concrete crushing (see Figures 5 and 6). The first vertical flexural crack initiated at the constant moment zone between the two loading points. Beyond the first cracking load, additional flexural cracks were developed within the constant moment zone. By increasing the load, flexural cracks became wider and propagated upward around the perimeter of the circular section, while some new cracks started to develop in the shear span. With further loading, the cracks formed along the shear span started to have some inclination towards the loading points. The specimen 8G20 continued to sustain more loads until the concrete crushing. The failure moment, M_n , was 264.08 kN.m for specimen 8G20. After concrete crushing, the specimen 8G20 continued to carry additional loads until the test has been stopped due to very high deformation or reaching the maximum displacement of the loading machine. This high level of the moment was named the peak moment. The peak moment, M_{peak} , was 358.58 kN.m. The ratio between M_{peak} and M_n was 135.8%. On the other hand, the early yielding of steel bars (failure moment) for specimen 8S20 prior to concrete crushing (peak moment) resulted in wider and concentrated cracks at the constant moment zone. The failure and peak moments for specimen 8S20 were 133.45 kN.m and 237.19 kN.m, respectively. After releasing the applied load at the end of the test, the GFRP RC specimen recovered most of their deflection during the unloading process, because GFRP bars in tension and compression sides of circular cross-section did not reach its rupture strain. While, during the unloading process of specimen 8S20, a permanent deflection was observed.

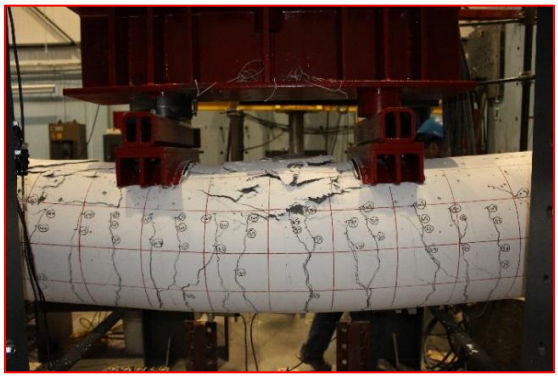

Figure 5 :Failure modes of Glass-FRP RC circular specimens (8G20).

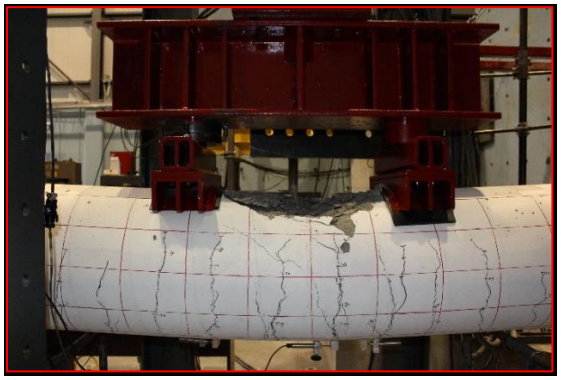

Figure 6: Failure modes of steel RC circular specimen (8S20).

Specimen ID	M_{cr} (kN.m)	M_n (kN.m)	M_{peak} (kN.m)	Failure mode[+]
8G20	24.15	264.08	358.58	C.C.
8S20	29.93	133.45	237.19	S.Y.

[+] C.C. = concrete crushing, S.Y. = steel yielding.

Table 3. Experimental moments, and mode of failure of tested specimens.

3 CONCLISIONS

In this paper, the flexural strength and behavior of circular concrete members reinforced with GFRP bars and spirals were investigated experimentally. Based on the experimental results presented in this paper, the following conclusions can be drawn:

1. The GFRP RC circular specimen behaved linearly until cracking and almost linearly between cracking and concrete crushing, with reduced stiffness. Interestingly, the specimen did not lose their load-carrying capacity after concrete crushing. Instead, they continued to sustain additional loads. This behavior can be attributed to the confinement effect provided by the GFRP bars and spirals that enhanced the specimen ductility and strength;
2. The failure of GFRP RC circular specimen occurred by concrete crushing, while the steel RC circular specimen failed due to steel yielding followed by concrete crushing;
3. The flexural strength at concrete crushing of GFRP-RC circular specimen was almost two times greater than that of steel-RC circular specimen at steel yielding with similar reinforcement ratio.

4 ACKNOWLEDGMENTS

The authors would like to express their special thanks and gratitude to the Ministère de l'Économie, de l'Innovation et des Exportations of Quebec, the Natural Science and Engineering Research Council of Canada (NSERC), the Fonds de recherche du Québec—Nature et Technologies (FQRNT), and Pultrall Inc. (Thetford Mines, Quebec) for their financial support. The authors thank the technical staff of the CFI structural laboratory in the Department of Civil Engineering at the University of Sherbrooke.

5 REFERENCES

[1] H. M. Mohamed, M. Z. Afifi, and B. Benmokrane. "Performance evaluation of concrete columns reinforced longitudinally with FRP bars and confined with FRP hoops and spirals under axial load." *J. Bridge Eng.*, Vol. 19, No. 7, 04014020, 2014.

[2] H. M. Mohamed and B. Benmokrane. "Design and performance of reinforced concrete water chlorination tank totally reinforced with GFRP bars: case study." *J. Compos. Constr.*, Vol. 18, No. 1, 05013001, 2014.

[3] American Concrete Institute (ACI) Committee 440. "*Guide for the design and construction of concrete reinforced with FRP bars.*" ACI 440.1R-15, Farmington Hills, MI., 2015.

[4] B. Benmokrane, O. Chaallal and R. Masmoudi. "Flexural response of concrete beams reinforced with FRP reinforcing bars." *ACI Struct. J.*, Vol. 93, No. 1, pp 46-55, 1996.

[5] M. Theriault and B. Benmokrane. "Effects of FRP reinforcement ratio and concrete strength on flexure behavior of concrete beams." *J. Compos. Constr.*, Vol. 2, No. 1, pp 7-16, 1998.

[6] M. A. Rashid, M. A. Mansur and P. Paramasivam. "Behavior of Aramid Fiber-Reinforced Polymer Reinforced High Strength Concrete Beams under Bending." *J. Compos. Constr.*, Vol. 9, No. 2, pp 117-127, 2005.

[7] C. Barris, L. I. Torres, A. Turon, M. Baena and A. Catalan. "An experimental study of the flexural behaviour of GFRP RC beams and comparison with prediction models." *Compos. Struct.*, Vol. 91, pp 286–295, 2009.

[8] C. Kassem, A. S. Farghaly and B. Benmokrane. "Evaluation of flexural behaviour and serviceability performance of concrete beams reinforced with FRP bars." *J. Compos. Constr.*, Vol. 15, No. 5, pp 682-695, 2011.

[9] A. El-Nemr, E. A. Ahmed and B. Benmokrane. "Flexural behavior and serviceability of normal- and high-strength concrete beams reinforced with glass fiber-reinforced polymer bars." *ACI Struct. J.*, Vol. 110, No. 6, pp 1077-1088, 2013.

[10] G. B. Maranan, A. C. Manalo, B. Benmokrane, W. Karunasena and P. Mendis. "Evaluation of the flexural strength and serviceability of geopolymer concrete beams reinforced with glass-fibre-reinforced polymer (GFRP) bars." *Eng. Struct.*, Vol. 101, pp 529–541, 2015.

[11] Canadian Standards Association (CSA). "*Design and construction of building components with fiber reinforced polymers.*" CAN/CSAS806-12, Rexdale, Ontario, Canada, 2012.

[12] Canadian Standards Association (CSA)."*Canadian highway bridge design code.*" CAN/CSA-S6-14, Rexdale, Ontario, Canada, 2014.

[13] G. S. R. Davalath and M. K. S. Madugula. "Analysis/design of reinforced concrete circular cross-sections." *ACI Struct. J.*, Vol. 85, No. 6, pp 617–623, 1988.

[14] T. Brøndum-Nielsen. "Ultimate flexure capacity of circular and annular cracked concrete sections." *ACI Struct. J.*, Vol. 85, No. 4, pp 437–441, 1988.

[15] E. Cosenza, C. Galasso and G. Maddaloni. "A simplified method for flexural capacity assessment of circular RC cross-sections." *Eng. Struct.*, Vol. 33, pp 942–946, 2011.

[16] M. Z. Afifi, H. M. Mohamed and B. Benmokrane. "Axial capacity of circular concrete columns reinforced with GFRP bars and spirals." *J. Compos. Constr.*, Vol. 18, No. 1, 04013017, 2014.

[17] M. Z. Afifi, H. M. Mohamed and B. Benmokrane. "Theoretical stress-strain model for circular concrete columns confined by GFRP spirals and hoops." *Eng. Struct.*, Vol. 102, pp 202–213, 2015.

[18] A. Hadhood, H. M. Mohamed and B. Benmokrane. "Axial load–moment interaction diagram of circular concrete columns reinforced with CFRP bars and spirals: experimental and theoretical investigations." *J. Compos. Constr.*, 04016092, 2016.

[19] A. H. Ali, H. M. Mohamed and B. Benmokrane. "Shear Strength of Circular Concrete Beams Reinforced with Glass Fiber-Reinforced Polymer Bars and Spirals." *ACI Struct. J.*, Vol. 114, No. 1, pp 39-49, 2017.